

Magnetic Characterization of 4 μm -thick Steel Made by Continuous Rolling Process for Power Electronic Applications in High Frequency

Nguyen Gia Minh Thao^{*a)} Member, Keisuke Fujisaki^{*} Senior member,
 Hiroaki Mamiya^{**} Non-member, Syuji Kuroda^{**} Non-member,
 Yoko Yamabe-Mitarai^{**} Non-member, Norie Motohashi^{**} Non-member

(Manuscript received Feb. 4, 2021, revised July 5, 2021)

This is the first study to experimentally perform the magnetic characterization of 4 μm -thick electrical steel sheet based on the sinusoidal excitation technique at high frequencies of up to 1 MHz. The steel is made of pure iron, fabricated using a high-precision continuous rolling process, which is a suitable and effective method for mass production. One ring core in which the steel part is appropriately fixed on a plastic cylindrical chassis is fabricated for measurements, whereas another ring core without the steel part is fabricated to serve as a reference. In addition, a method for effectively estimating the magnetic flux density and relative permeability of the steel part in the first ring core from the measured data of the two ring cores is presented as a key contribution of this study. This method can also be applied in the magnetic characterization of other thin steels at high frequencies. The magnetic flux density–field intensity (B – H) curve, relative permeability, and iron loss per weight of the examined 4 μm -thick steel are measured and evaluated through experiments. The measured results and Steinmetz approximation indicate that the eddy current loss in the investigated steel is relatively considerable at high frequencies of 500 kHz and above.

Keywords : 4 μm -thick steel, continuous rolling process, high frequency, magnetic characterization, measurement method, ring core

Nomenclature

$B_{\text{Ring1,m}}$	Maximum magnetic flux density of first ring core
$B_{\text{Ring2,m}}$	Maximum magnetic flux density of second ring core
$B_{\text{Ring1,c}}$	Magnetic retentivity of first ring core
$B_{\text{Ring2,c}}$	Magnetic retentivity of second ring core
$H_{\text{Ring1,m}}$	Magnetic field intensity of first ring core
$H_{\text{Ring2,m}}$	Magnetic field intensity of second ring core
$H_{\text{Ring1,c}}$	Magnetic coercivity of first ring core
$H_{\text{Ring2,c}}$	Magnetic coercivity of second ring core
S_{Ring1}	Cross sectional area of first ring core
S_{Ring2}	Cross sectional area of second ring core
Φ_{Ring1}	Magnetic flux of first ring core including steel part
Φ_{Ring2}	Magnetic flux of second ring core without steel part
$B_{\text{Fe1,m}}$	Maximum magnetic flux density through steel part in first ring core
$\mu_{\text{Fe1,r}}$	Relative permeability of steel part in first ring core
l_{Fe1}	Magnetic length of steel part in first ring core
N_1	Number of turns of primary copper coil
N_2	Number of turns of secondary copper coil
I_1	Primary input current of ring core
V_2	Secondary open-circuit voltage of ring core
P_{cm}	Measured iron loss per weight

1. Introduction

The development, magnetic properties and evaluation of several recent non-oriented steels effectively used for electrical motors and

various applications at high frequencies were presented⁽¹⁾. Furthermore, an appropriately fine-tuning technique for the hot rolling temperatures, ranges of the chemical composition and strip tension values in the making process to significantly enhance the magnetic properties of a reversible grain-oriented steel was proposed and evaluated⁽²⁾. Besides, a novel technical scheme for efficiently fabricating the electrical sheets of Fe-6.5wt%Si alloy with a compact and suitable process was developed and assessed⁽³⁾.

On the other hand, a unique scheduling issue based on the single-machine type, that comprehensively considered the setting-up time based on the order, release time, and restraints of the due time for optimally scheduling a wire rod and bar rolling process in the steel factories, was implemented⁽⁴⁾. In addition, a calculation model and identification process suitably based on the finite element analysis and the consistent thermodynamic theory for effectively estimating the characteristics of iron losses in non-grain-oriented steels at the high frequencies and wide range of the magnetic field strength are researched and developed⁽⁵⁾. According to an experimental analysis and investigation⁽⁶⁾, the supply of high frequency harmonics into a toroidal magnetic circuit using the non-oriented electrical steel laminations may help to decrease the low-frequency iron losses of the considered magnetic circuit. Moreover, μm -thick electrical steels made by the continuous rolling process have been promising materials possibly utilized for the magnetic inductor and transformer cores in power-electronic applications at high frequencies as well as for mass production⁽⁷⁾.

The authors⁽⁸⁾ proposed a unique design method for magnetic components used in a high-efficiency bidirectional DC-DC three-port converter prototype, which can reduce around 10% in the size of the magnetic components and 30% in the overall size of the considered converter than that with the conventional design technique. Furthermore, a play model was designed to analyze the

This paper is based on Reference (27), which published in the International Conference ICEMS (2020) ©2020 IEEJ.

a) Correspondence to: Nguyen Gia Minh Thao. E-mail: nguyen.thao@toyota-ti.ac.jp

* Toyota Technological Institute
 2-12-1, Hisakata, Tenpaku ward, Nagoya city, Aichi prefecture,
 468-8511, Japan

** National Institute for Materials Science
 1 Chome-1 Namiki, Tsukuba city, Ibaraki, 305-0044, Japan

iron loss of reactor core utilized in DC-DC converter with detailed considerations of the hysteresis B - H curve⁽⁹⁾. A novel design for the cores of induction heating coils with the significant decrease of iron loss, which was applied for a small-foreign-metal particle detector using a high-frequency SiC-MOSFET inverter with the carrier frequency of 400 kHz, was also introduced and evaluated⁽¹⁰⁾. Besides, the characteristics and parasitic capacitance of small-size toroidal reactors at high frequencies were analyzed and assessed to be noticeably affected by the wire guides and resin materials⁽¹¹⁾.

The flaky-shaped thin powders were developed and evaluated⁽¹²⁾⁻⁽¹⁴⁾ with fairly good magnetic properties, and can be used for power electronics applications at high frequencies. However, the manufacturing of flaky-shaped thin powders for mass commercial production is relatively difficult. Moreover, a unique method to measure the conductivity and relative permeability of 0.1–0.25 mm-thick steels was proposed⁽¹⁵⁾. Another study⁽¹⁶⁾ investigated the 0.18 mm-thick steel, and 0.08 mm-thick steel⁽¹⁷⁾ was also examined.

The 50 μ m thin steels of Nd-(FeCoNiTi)-B sintered magnets⁽¹⁸⁾ and 30 μ m-thick grain-oriented silicon steel⁽¹⁹⁾ were introduced and investigated. Besides, the production of 5–8 μ m grain-oriented silicon steel sheets was discussed⁽²⁰⁾ without the consideration of effects of the high excitation frequency on those steels' magnetic characteristics. Toyo Kohan Co., Ltd. in Japan has recently produced the commercial cold-rolled steel sheet with a thickness of 25 μ m⁽²¹⁾. In fact, there have been no studies on the magnetic properties and details of related measurement method of μ -class electrical steel at high excitation frequencies of up to $f = 1$ MHz.

Hence, the key originality of our research is on the combination of the production of the 4 μ m-thick steel fabricated from pure iron using the rolling process and the measurements of its magnetic properties at high frequencies up to 1 MHz. Moreover, procedures and details of the proposed measurement method are described, which can be applied in the magnetic characterization of other thin steels at high frequencies. In fact, our measurement method has not yet been presented in detail in other existing studies and catalogues. In addition, our 4 μ m-thick steel considered in this study is made of pure iron, which is different with the μ -class grain-oriented silicon steels^{(19),(20)} produced from the silicon iron alloys.

Furthermore, this paper focuses on the use of the continuous rolling process to make the 4 μ m-thick steel sheet because the rolling process is particularly convenient for the mass production of related commercial products and applications. Besides, our ultimate research goal will be to design and fabricate magnetic inductor cores using the thin steel for power electronics converters in electric vehicles (EVs), which can efficiently operate at a large power up to tens of kW and high frequencies of MHz with a reasonable cost. In this case, the rolling process is also suitable among the fabrication methods of μ -thick steels. Moreover, the maximum magnetic flux density through the considered steel part in this study is $B_{Fe1,m} = 0.262$ T at a peak frequency of 1 MHz, while some existing studies^{(13),(14)} investigated with only a small $B_{Fe,m}$ at high frequencies; in detail, $B_{Fe,m} = 3$ mT⁽¹³⁾ at $f = 1$ MHz, and $B_{Fe,m} = 50$ mT⁽¹⁴⁾ at $f = 100$ kHz. Due to the nonlinearity of magnetic properties especially at high frequencies up to 1 MHz, the detailed measurement and evaluation of magnetic properties with a fairly high flux density is helpful. These are the main motivation and usefulness of our study.

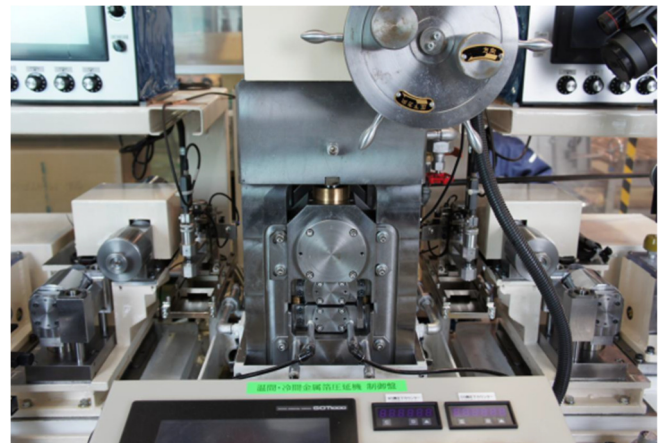
Dimensions of the considered steel sheet and two ring cores under test are expressed in Section 2. Furthermore, the proposed measurement method and procedure utilized in experiments are

described in Section 3 as another significant contribution of this study. In addition, the measured results of B - H curves, relative permeability and iron loss per weight as well as the Steinmetz-based formula to relatively estimate the characteristics of the iron loss are shown in Section 4; discussions are also presented in the section. Last, the conclusions and future work are included in Section 5.

2. Descriptions of 4 μ m-thick Steel Sheet and Two Ring Cores for Measurement

Firstly, an electrical steel made of pure iron was conventionally cold-rolled to a sheet with a thickness of 200 μ m and annealed in vacuum. After that, the 4 μ m-thick steel sheet was formed by the continuous rolling process using the mill with twelve rolls structured in a vertically split type as illustrated in Fig. 1 panel (a). Furthermore, in the production and rolling process, a specialized measurement equipment as depicted in Fig. 1 panel (b) was used to carefully check and confirm the thickness of the steel sheet. Regarding all samples fabricated in this research, the material in use (i.e. pure iron) and the manufacturing procedures are entirely same as well as the thickness of each sample is strictly checked as 4 μ m.

Details of the 4 μ m-thick steel sheet and first ring core used in measurements are described in Fig. 2. The total length of the steel part attached in the first ring core as presented in Fig. 2 panel (a) is $l_{Fe1} = 0.712$ m. As shown in the central part of Fig. 2 panel (b), firstly, the steel sheet is appropriately affixed to an insulation using a very small amount of glue or adhesive tape; the commercial insulation of Kapton® 20EN⁽²²⁾ with a thickness of 5 μ m is used in this study. Then, the steel part together with the insulation⁽²²⁾ is attached on a plastic cylindrical chassis as shown in the right part of Fig. 2 panel (b). In total, there are ten rounds of the 4 μ m-thick steel together with the insulation as described in the right part of Fig. 2 panel (c).



(a) Continuous rolling process equipment



(b) Measurement equipment of thickness

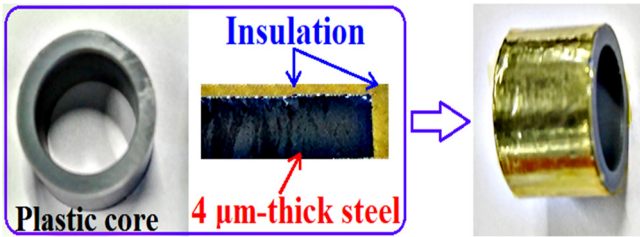
Fig. 1. Equipment for making 4 μ m-thick steel sheet in this study

As depicted in Fig. 2 panel (c), the cross section of a ring core is covered and indicated by the frame ABCD; we note that the area of the frame ABCD is equal to the sum of areas of the two frames AEFD and EBCF, i.e. $S_{ABCD} = S_{AEFD} + S_{EBCF}$. In the first ring core, the material of the chassis section covered by the frame AEFD is plastic, and the remaining section limited by the frame EBCF is the investigated steel part together with the insulation⁽²²⁾. As shown in the central and right parts of Fig. 2 panel (b), the insulation is yellow.

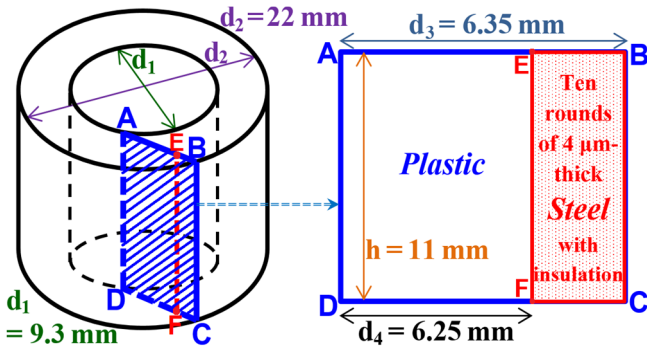
In addition, another plastic ring core without a steel part, which has the same dimension and number of turns of copper coils with that of the first ring core (with the steel part) as presented in Fig. 3, is used to measure the maximum magnetic flux of the non-steel ring core $\Phi_{\text{Ring2,m}}$ under the similar maximum magnetic field intensity with the first ring core, i.e. $H_{\text{Ring1,m}} = H_{\text{Ring2,m}}$. In detail, in the second ring core as given by the right part of Fig. 3, the material of the chassis section covered by the frame AEFD as shown in Fig. 2 panel (c) is still plastic, but the remaining section limited by the frame EBCF comprises only the insulation⁽²²⁾ without a steel part. Besides, the numbers of turns of the primary and secondary copper coils of the two ring cores are same as $N_1 = N_2 = 44$. The ultimate aim is to efficiently estimate the magnetic flux density through the considered steel part $B_{\text{Fe1,m}}$ in the first ring core and its relative permeability $\mu_{\text{Fe1,r}}$ in measurements and calculation.



(a) 4 μ m-thick steel sheet



(b) Steel part and insulation fixed on a plastic cylindrical chassis



(c) Dimension of first ring core with steel part

Fig. 2. Details of 4 μ m-thick steel sheet and first ring core



Fig. 3. Two ring cores with same dimension and number of turns of copper coils; *left*: first ring core with considered steel part; *right*: second ring core without steel part

3. Proposed Measurement Method in Experiments

As described in Fig. 4, a 16-bit full-automatic B - H analyzer SY-8219 together with a measurement pod SY-955 from Iwatsu⁽²³⁾ is utilized for accurate measurements under the sinusoidal excitation technique with different excitation frequencies from $f = 10, 100, 200, 300$ kHz and up to 1 MHz. The maximum magnetic flux density of the first ring core is always fixed at $B_{\text{Ring1,m}} = 2$ mT in measurements. Firstly, the secondary open-circuit voltage V_2 and the input primary current I_1 of the ring core are measured to calculate B and H as expressed in (1) and (2), respectively; after that, the iron loss per weight P_{cm} is computed according to (3).

$$B = \frac{1}{N_2 S} \int V_2 dt \quad (1)$$

$$H = \frac{N_1 I_1}{l} \quad (2)$$

$$P_{\text{cm}} = \frac{f}{\rho W_m} \int H dB \quad (3)$$

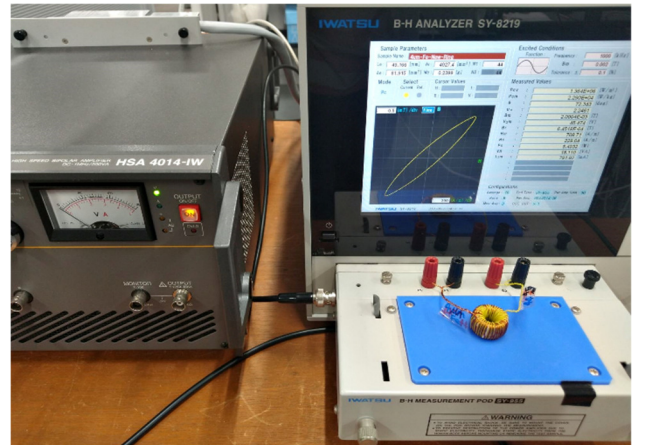


Fig. 4. Measurement system including a B - H analyzer and linear amplifier with excitation frequency up to 1 MHz

Where ρ and W_m are the density and weight of the steel part, respectively; S is the cross sectional area; l is the magnetic length of the ring core, and f is the excitation frequency.

In this study, the proposed measurement method and procedure have three main steps in the order as follows.

Step 1: The first ring core with the 4 μ m-thick steel part is connected to the B - H analyzer SY-8219 from Iwatsu for measurement as depicted in Fig. 4. In this step, the peak magnetic flux density of this ring core is always fixed at $B_{Ring1,m} = 2$ mT, where the excitation frequency is altered from $f = 10, 100, 200, 300$ kHz and up to 1 MHz. At each frequency, the maximum magnetic field intensity $H_{Ring1,m}$ of this ring core is measured and collected as shown in the upper part of Table 1.

Step 2: The first ring core is removed from the B - H analyzer. After that, the second ring core without the steel part is now connected to the B - H analyzer for another measurement. In this case, the maximum magnetic field intensity $H_{Ring2,m}$ of the second ring core is set to be equal to $H_{Ring1,m}$ of the first ring core (already measured in Step 1) at each excitation frequency of $f = 10, 100, 200, 300$ kHz and up to 1 MHz as described in the lower part of Table 1. At each excitation frequency, the maximum magnetic flux density $B_{Ring2,m}$ of the second ring core (without the steel part) is measured and collected.

In addition, all the setting values and measured data in Step 1 and Step 2 are presented in Table 1 for easier to understand the detailed procedures of the proposed measurement method. In this table, we note that the magnetic flux density $B_{Ring1,m}$ is the setting value for the first ring core measured in Step 1, while the magnetic field intensity $H_{Ring2,m}$ is the setting value for the second ring core performed in Step 2; the other values such as $B_{Ring1,c}$, $H_{Ring1,m}$, $H_{Ring1,c}$, $B_{Ring2,m}$, $B_{Ring2,c}$ and $H_{Ring2,c}$ are the measured data of the two ring cores.

Step 3: From the six determined parameters $B_{Ring1,m}$, $H_{Ring1,m}$, S_{Ring1} , $B_{Ring2,m}$, $H_{Ring2,m}$ and S_{Ring2} , where $S_{Ring1} \approx S_{Ring2}$ and $H_{Ring1,m} = H_{Ring2,m}$, the maximum magnetic flux density through the considered steel part $B_{Fe1,m}$ and its relative permeability $\mu_{Fe1,r}$ in the first ring core at each excitation frequency can be estimated according to (4)-(7).

$$\Phi_{Ring1,m} \approx \Phi_{Fe1,m} + \Phi_{Ring2,m} \quad (4)$$

Where $\Phi_{Ring1,m}$, $\Phi_{Fe1,m}$, and $\Phi_{Ring2,m}$ are the maximum magnetic flux of the first ring core, the investigated steel part in the first ring core, and the second ring core without a steel part, respectively.

Equation (4) can be rewritten as follows

$$B_{Fe1,m} \cdot S_{Fe1} \approx B_{Ring1,m} \cdot S_{Ring1} - B_{Ring2,m} \cdot S_{Ring2} \quad (5)$$

Where S_{Ring1} , S_{Fe1} , and S_{Ring2} are the cross sectional areas of the first ring core, the steel part in the first ring core, and the second ring core without a steel part, respectively.

After that, $B_{Fe1,m}$ of the investigated steel part in the first ring core can be computed as

$$B_{Fe,m} \approx \frac{B_{Ring1,m} \cdot S_{Ring1} - B_{Ring2,m} \cdot S_{Ring2}}{S_{Fe1}} \quad (6)$$

where $S_{Ring1} \approx S_{Ring2}$, and $H_{Ring1,m} = H_{Ring2,m}$.

From (6), the relative permeability of the steel is determined as

$$\mu_{Fe1,r} = \frac{B_{Fe1,m}}{\mu_0 H_{Ring1,m}} \quad (7)$$

where $\mu_0 = 4\pi \times 10^{-7}$ H/m.

4. Experimental Results and Discussions

4.1. Experimental Results

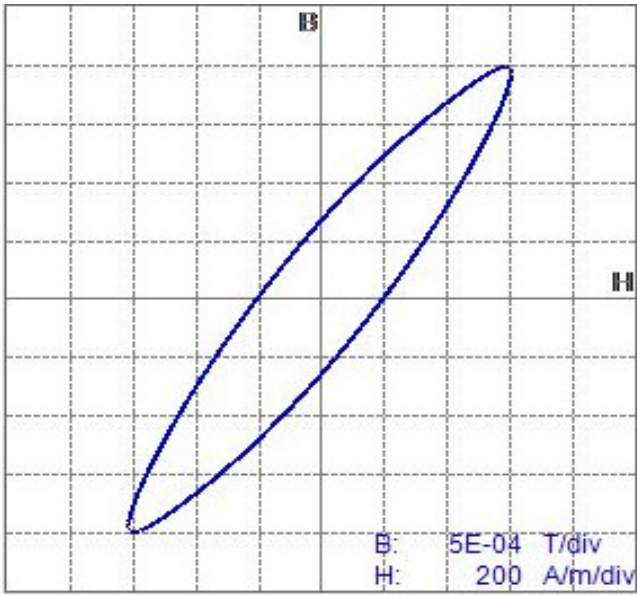
From the output direct data of the B - H analyzer Iwatsu SY-8219, the measured B - H curves of the first ring core (with the considered steel part) and the second ring core (without a steel part) at the peak excitation frequency of $f = 1$ MHz are expressed in Fig. 5 panels (a) and (b), respectively, where the maximum magnetic field strength values of the two ring cores are same, i.e. $H_{Ring1,m} = H_{Ring2,m} = 610.7$ A/m. From this figure and Table 1, we can recognize the significant differences between the measured B - H curves of the two ring cores.

In addition, the measured B - H curve of the first ring core with the steel part varies remarkably once the excitation frequency rises as shown in Fig. 6. This indicates that the iron loss of the steel part may considerably increase when the excitation frequency increases.

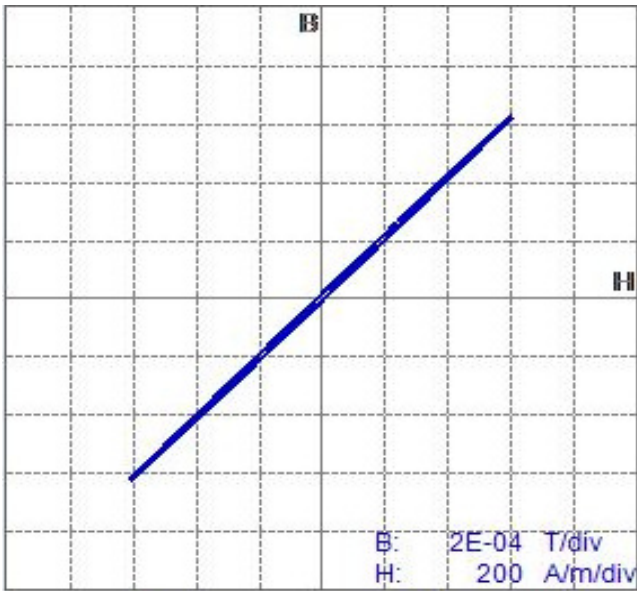
From (6) and (7), the maximum magnetic flux density $B_{Fe1,m}$ and the relative permeability $\mu_{Fe1,r}$ of the steel part in the first ring core are estimated within the value ranges of $B_{Fe1,m} = 0.267$ – 0.262 T and $\mu_{Fe1,r} = 386.8$ – 341.4 , respectively, where the excitation frequency is varied from 10 kHz to 1 MHz as described in Fig. 7. We can see that the estimated $B_{Fe1,m}$ of the steel part is almost constant as illustrated by the purple solid line in Fig. 7 for good evaluation. Moreover, the measured results of the iron loss per weight P_{cm} of the examined steel part in the first ring core are presented in Fig. 8.

Table 1. Setting values and measured data in Step 1 and Step 2 of proposed measurement method

Excitation frequency f		10 kHz	100 kHz	200 kHz	300 kHz	400 kHz	500 kHz	600 kHz	700 kHz	800 kHz	900 kHz	1 MHz
First ring core (with steel part), in Step 1	$B_{Ring1,m}$ [mT] (setting value)	2	2	2	2	2	2	2	2	2	2	2
	$B_{Ring1,c}$ [mT]	0.506	0.56	0.57	0.58	0.589	0.6	0.61	0.62	0.637	0.649	0.664
	$H_{Ring1,m}$ [A/m]	545.2	558.4	571.7	579	585.8	590.2	592.9	598	602.8	607.9	610.7
	$H_{Ring1,c}$ [A/m]	132.1	152.5	160.1	164.8	170.5	175.6	179.8	184.6	189	196.3	202.6
Second ring core (without steel part), in Step 2	$B_{Ring2,m}$ [mT]	0.6174	0.6034	0.6035	0.605	0.6097	0.613	0.6152	0.6159	0.6206	0.6258	0.629
	$B_{Ring2,c}$ [mT]	6.72×10^{-3}	27.3×10^{-3}	22.2×10^{-3}	18.1×10^{-3}	16×10^{-3}	14.7×10^{-3}	13.8×10^{-3}	13.1×10^{-3}	12.5×10^{-3}	12×10^{-3}	11.5×10^{-3}
	$H_{Ring2,m}$ [A/m] $= H_{Ring1,m}$ (setting value)	545.2	558.4	571.7	579	585.8	590.2	592.9	598	602.8	607.9	610.7
	$H_{Ring2,c}$ [A/m]	5.93	25.16	20.79	17.15	15.26	13.91	12.99	12.12	11.66	11.61	10.89



(a) First ring core with examined steel part, where $B_{\text{Ring1,m}} = 2 \text{ mT}$



(b) Second ring core without steel part, where $H_{\text{Ring2,m}} = H_{\text{Ring1,m}}$

Fig. 5. Measured B - H curves of two ring cores obtained from analyzer Iwatsu SY-8219, at $f = 1 \text{ MHz}$

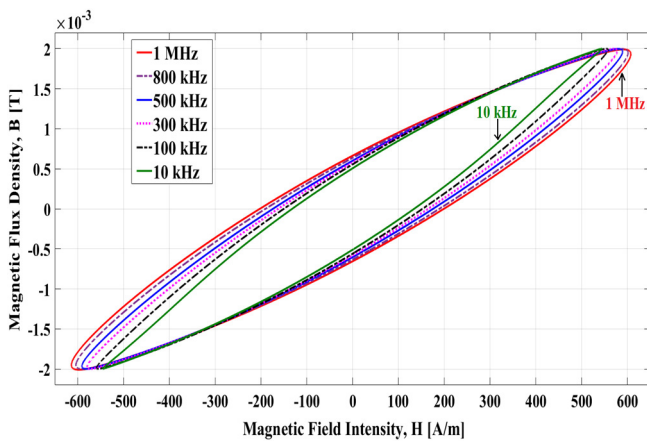


Fig. 6. Measured B - H curves of first ring core with steel part attached, in Step 1 of measurement procedure

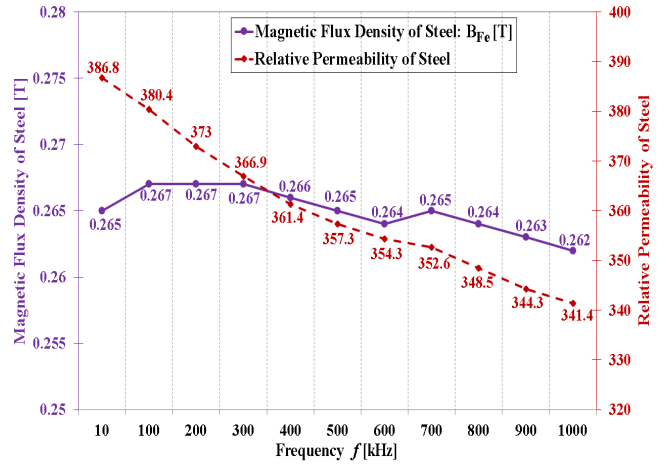


Fig. 7. Experimental results of $B_{\text{Fe1,m}}$ and $\mu_{\text{Fe1,r}}$ of considered steel

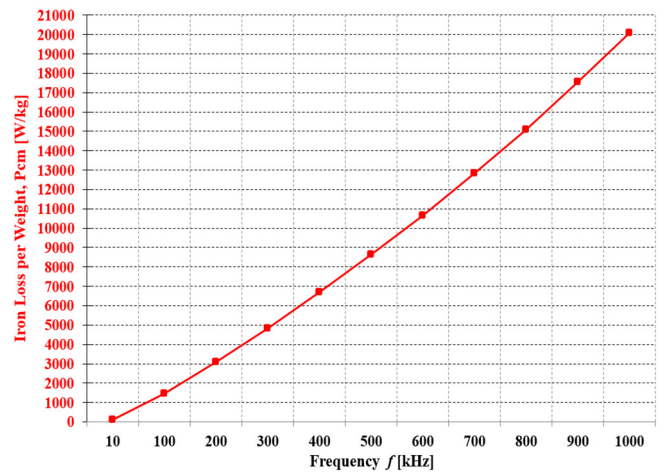


Fig. 8. Measured results of P_{cm} of tested steel with $B_{\text{Fe1,m}}$ in Fig. 7

Moreover, by using (4)-(6) with additional measurements, the response of the magnetic flux density of the steel part $B_{\text{Fe1,m}}$ in the first ring core under alterations in the magnetic field intensity H is expressed in Fig. 9, where H with the first and second ring cores in each experiment is same ($H_{\text{Ring1,m}} = H_{\text{Ring2,m}}$), and the frequency is 1 MHz. Due to the current limit of the linear amplifier HSA 4014-IW (Fig. 4), H is varied from 5 to 2200 A/m in these measurements.

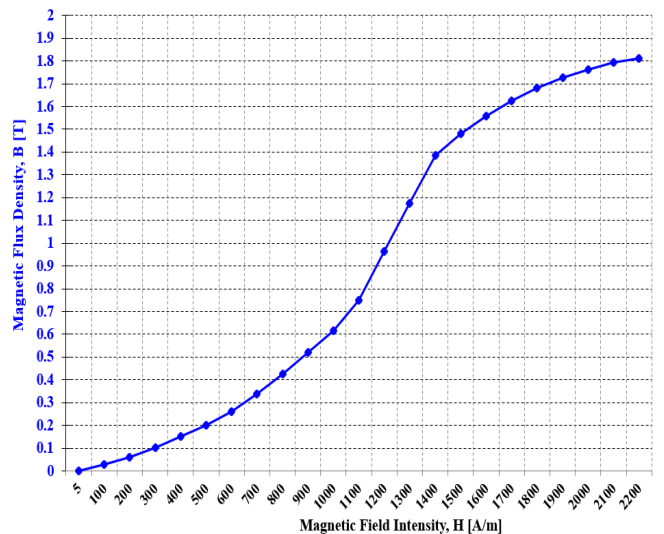


Fig. 9. Response of $B_{\text{Fe1,m}}$ of considered steel under changes in H

Furthermore, the ratio value δ_Φ of the magnetic flux Φ between the second and first ring cores (Fig. 3) in experiments is computed according to (8). The main aims of calculating the value of δ_Φ are to thoroughly know and monitor the ratio of the magnetic flux of the second ring core (without a steel part) compared to that of the first ring core (with the steel part attached) at the same magnetic field intensity under large changes in the excitation frequency. In this paper, the value of δ_Φ slightly varies in a range of 30.1–31.5% once the frequency considerably changes from $f=10$ kHz to 1 MHz. On the other hand, if the actual value of δ_Φ changes very significantly when the excitation frequency alters, we should carefully recheck the measurement procedures and results as well as need to measure again with another sample of the first ring core consisting of the steel part for validation.

$$\delta_\Phi = \frac{\Phi_{Ring2}}{\Phi_{Ring1}} \times 100\% \quad (8)$$

From Fig. 8, the iron loss per weight and frequency is varied in the range of $P_{cm}/f = 12.2\text{--}20.06$ W/kg/kHz, when the frequency is changed in the range of $f=10$ kHz – 1 MHz as described in Fig. 10.

4.2. Steinmetz-based Estimation of Iron Loss per Weight and Discussions on Measured Results

With the proper use of the *fit* command in MATLAB⁽²⁴⁾, the conventional Steinmetz-based formula for relatively estimating the hysteresis and eddy current loss components in the measured P_{cm} of the investigated steel as illustrated by Fig. 8 can be expressed as

$$P_{cm} = P_{hys} + P_{eddy} = k_{hys} B_{Fe1,m}^2 f + k_{eddy} B_{Fe1,m}^2 f^2 \quad (9)$$

where $B_{Fe1,m} = 0.262$ T, $k_{hys} = 0.206$ and $k_{eddy} = 8.7 \times 10^{-8}$ in this study.

The detailed comparison between the measured data of P_{cm} and the Steinmetz-based estimation given by (9) is depicted in Fig. 11, where $B_{Fe1,m} = 0.262$ T (Fig. 7). For analysis purpose, the ratio η_{est} between the estimated eddy current loss P_{eddy} and hysteresis loss P_{hys} is computed by (10), and its values are represented in Table 2.

$$\eta_{est} = \frac{P_{eddy}}{P_{hys}} \times 100\% \quad (10)$$

As shown in (9), Fig. 11, and Table 2, at the low frequency of 10 kHz, the hysteresis loss is dominant while the eddy current loss is very tiny. When the frequency f increases from 10 kHz to 100 kHz as ten times of change, the increasing rate of the eddy current loss is proportional to f^2 as hundred times, while the increasing rate of the hysteresis loss is proportional to the frequency as only ten times. In addition, for the frequency range of $f=100$ kHz – 1 MHz, the step change of frequency is 100 kHz which is equivalent to only an increase of 200% – 11.1%; hence, the rise of P_{cm}/f in this case is much reduced than that with $f=10\text{--}100$ kHz. Moreover, once the

frequency increases, effects of the eddy current in the steel become more substantial^{(13),(14)} as depicted in Fig. 11. These are the reasons why the variation of P_{cm}/f for the frequency range of $f=10\text{--}200$ kHz is more nonlinear than that for $f=200$ kHz – 1 MHz as shown in Fig. 10. The nonlinearity in the variation of the iron loss per frequency is also observed with the flaky-shaped powder⁽¹⁴⁾.

From Table 2, we can see that the ratio η_{est} between the estimated eddy current loss P_{eddy} and hysteresis loss P_{hys} at a low frequency of 10 kHz is very small as 0.43%. Although the measured P_{cm}/f increases fairly linearly for the frequency range of $f=100$ kHz – 1 MHz as shown in Fig. 10, η_{est} is still small in a range of 4.22–16.89% for the frequency range of $f=100\text{--}400$ kHz as presented in the last row of Table 2. Meanwhile, when the frequency is from $f=500$ kHz to 1 MHz, the estimated value of η_{est} becomes 21.12% to 42.23%, which are relatively substantial. These quantitative data demonstrate that the eddy current loss is comparatively significant in the investigated steel at the high excitation frequencies from 500 kHz and above as also illustrated by the purple solid line in Fig. 11.

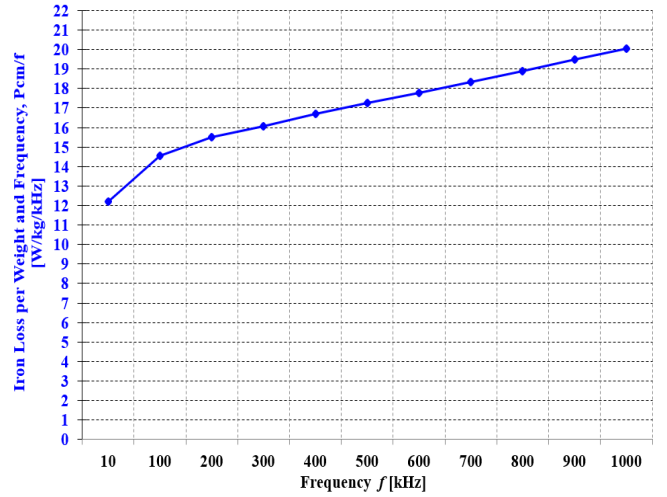


Fig. 10. Experimental results of P_{cm} per frequency of steel, P_{cm}/f

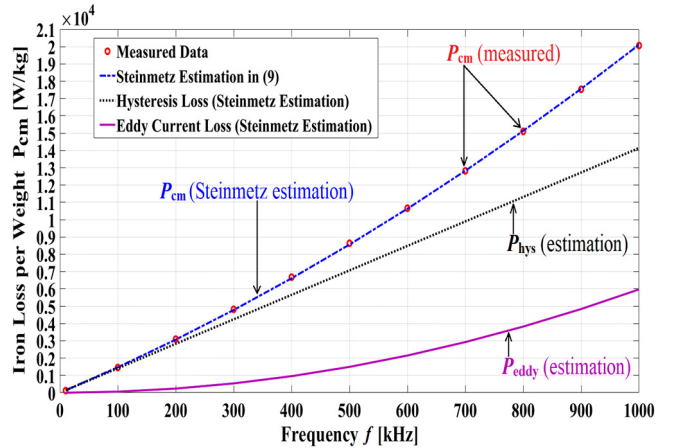


Fig. 11. Measured data and Steinmetz-based estimation of P_{cm}

Table 2. Ratio between estimated eddy current and hysteresis losses of steel using Steinmetz formula, where $B_{Fe1,m} = 0.262$ T

Excitation frequency f	10 kHz	100 kHz	200 kHz	300 kHz	400 kHz	500 kHz	600 kHz	700 kHz	800 kHz	900 kHz	1 MHz
Hysteresis loss P_{hys} [W]	141	1414	2828	4242	5656	7070	8484	9898	11313	12727	14141
Eddy current loss P_{eddy} [W]	0.6	59.7	238.9	537.5	955.5	1493	2149.9	2926.3	3822.1	4837.3	5972
Ratio value η_{est} [%]	0.43	4.22	8.45	12.67	16.89	21.12	25.34	29.56	33.79	38.01	42.23

Owing to the remarkable effects of the eddy current at high frequencies^{(13),(25)}, the relative permeability $\mu_{Fe1,r}$ of the thin steel considered in this paper is slightly decreased from 386.8 to 341.4 when the excitation frequency increases from $f = 10$ kHz to 1 MHz as presented by the dashed line in Fig. 7.

Since there are differences in the materials, fabrication methods and test conditions in use between this paper and other existing related studies, the relative permeability values of only the iron powders^{(13),(14)} and thin materials⁽¹⁵⁾ are used to briefly compare with that of the investigated 4 μ m-thick steel in this study for reference purpose. In detail, the relative permeability values of the spherical and flake powder cores⁽¹³⁾ at $f = 1$ MHz are 15 and 67, respectively, where the maximum magnetic flux density B_m used in measurement is 3 mT; the relative permeability of the flake-shaped iron powder MG150D⁽¹⁴⁾ at $f = 1$ MHz is around 64, where this powder core sample was compacted at 686 MPa. Besides, the 0.25 mm-thick Fe-based material⁽¹⁵⁾ has a relative permeability as around 90 at $f = 100$ kHz, while that of the 0.1 mm-thick Ni-based material⁽¹⁵⁾ is in a range of 14–11 for a frequency range of $f = 100$ kHz – 1 MHz. From the above observations, $\mu_{Fe1,r} = 341.4$ at the high frequency of 1 MHz of the considered 4 μ m-thick steel is relatively acceptable compared to that of some existing thin materials^{(13)–(15)}. In next study, other thin steels^{(20),(26)} will be assessed and compared.

An insulation material is usually a non-magnetic material and can effectively prevent the transmission of electricity. Thus, in ideal situation, there are no significant effects of the insulation material in use (Kapton® 20EN⁽²²⁾) on the measured magnetic properties of the tested steel. However, in the authors' opinions, the following points have to be considered in experiments and measurements. Firstly, the temperature in the first ring core including the steel part together with the insulation may significantly increase during the consecutive experiments and measurements, which may impact the measured magnetic properties of the steel if the temperature is high enough. In fact, different insulation materials often have dissimilar influences on the increase of the temperature in the first ring core. Hence, to effectively prevent the high rise of the temperature in the first ring core in experiments, an appropriate insulation material with good thermal characteristics⁽²²⁾ should be utilized, as well as the time between the two consecutive measurements of the ring core should be at least five minutes according to our experience.

Furthermore, as described in the second paragraph of Section 2 and Fig. 2 panels (b) and (c), when we manually make the first ring core consisting of the steel part affixed to the insulation and then wind the two copper coils on the ring core, some small pressure or stress may occur and influence the steel part, that may also cause the unexpected effect on the measured magnetic characteristics of the investigated steel. Therefore, to mitigate this issue, during the manual manufacturing and coiling of the first ring core, we should perform properly, slowly and carefully. Finally, the thickness of the insulation material should be suitably selected according to the thickness of the considered steel sheet. In the experimental ring core, the insulation material affects the actual total thickness of the area indicated by the frame EBCF as shown in Fig. 2 panels (b) and (c). If the thickness of the insulation material is very much larger than that of the examined steel, the estimated ratio between the magnetic flux values through the insulation part and the steel part in the first ring core will increase remarkably, which may impact the measured magnetic properties of the steel. For example, when the thickness of the steel is 4 μ m as considered in this study, the thickness of the insulation material can be chosen in a range of around 4–12 μ m

according to our experience and thought. The particular effects of different insulation materials and their thickness on the measured magnetic properties of μ m-thick steels at high frequencies will be thoroughly investigated, analyzed and assessed in future research.

5. Conclusion

This paper has comprehensively evaluated the magnetic characteristics of the 4 μ m-thick electrical steel, where it is made of pure iron by using the continuous rolling process and the excitation frequency is altered from $f = 10, 100, 200, 300$ kHz and up to 1 MHz in experiments. In detail, the B - H curve, iron loss per weight, relative permeability, and detailed characteristics of the hysteresis and eddy current loss components based on the Steinmetz estimation of the steel have been examined and assessed. Furthermore, an efficient measurement method with the proper utilization of another non-steel ring core with the same dimension and copper coils to the first ring core was introduced for appropriately determining the maximum magnetic flux density $B_{Fe1,m}$ and relative permeability $\mu_{Fe1,r}$ of the considered steel part attached in the first ring core. Besides, this measurement method can be appropriately applied to evaluate the high-frequency magnetic properties of other thin electrical steels.

At the maximum magnetic flux density of $B_{Fe,m} = 0.262$ T and the peak excitation frequency of $f = 1$ MHz, the estimated relative permeability and iron loss per weight of the steel part in the first ring core are $\mu_{Fe1,r} = 341.4$ and $P_{cm} = 20063$ W/kg, respectively. Moreover, the results in Figs. 10 and 11 and the estimated ratio η_{est} in Table 2 have demonstrated that the eddy current loss component in the 4 μ m-thick steel is relatively substantial once the excitation frequency is from 500 kHz and above. Therefore, this steel may be utilized for magnetic inductor and transformer cores in various power electronic applications at high frequencies with the relatively good performance. Some extra research and improvement in continuing to reduce the iron loss for this steel is also recommended for the implementation.

In future work, the magnetic characteristics of the 4 μ m-thick steel examined in this paper will be compared with that of another 3.8 μ m-thick amorphous material in finite element analysis and experiments. Furthermore, effects of the eddy current maybe caused by the copper coils wound on the ring cores at high frequencies will be investigated in detail.

References

- (1) Y. Oda, T. Okubo, and M. Takata: "Recent development of non-oriented electrical steel in JFE Steel," JPE Technical Report, no. 21, pp. 7-13, 2016.
- (2) M. C. Guimaraes, F. L. Alcantara, R. U. C. Moreira, N. E. F. Lima, and J. G. Ank: "Improvement of magnetic properties of a reversible hot rolled grain-oriented electrical steel," IEEE Transactions on Magnetics, vol. 52, no. 5, paper ID: 2002704, 2016.
- (3) J. Xie, H. Pan, H. Fu, and Z. Zhang: "High efficiency warm-cold rolling technology of Fe-6.5wt%Si alloy sheets," Procedia Engineering, vol. 81, pp. 149-154, 2014.
- (4) Z. Zhao, S. Liu, M. Zhou, X. Guo, and L. Qi: "Decomposition method for new single-machine scheduling problems from steel production systems," IEEE Transactions on Automation Science and Engineering, vol. 17, no. 3, pp. 1376-1387, 2019.
- (5) F. Henrotte, S. Steentjes, K. Hameyer, and C. Geuzaine: "Iron loss calculation in steel laminations at high frequencies," IEEE Transactions on Magnetics, vol. 50, no. 2, paper ID: 7008104, 2014.
- (6) L. Petrea, C. Demian, J. F. Brudny, and T. Belgrand: "High-frequency harmonic effects on low-frequency iron losses," IEEE Transactions on Magnetics, vol. 50, no. 11, paper ID: 6301204, 2014.
- (7) M. Komatsubara, K. Sadahiro, O. Kondo, T. Takamiya, and A. Honda: "Newly developed electrical steel for high-frequency use," Journal of Magnetism & Magnetic Materials, vol. 242-245, pp. 212-215, 2002.
- (8) S. Inoue, K. Itoh, M. Ishigaki, and T. Sugiyama: "Integrated magnetic component of a transformer and a magnetically coupled inductor for a three-

- port DC-DC converter," IEEJ Journal of Industry Applications, vol. 9, no. 6, pp. 713-722, 2020.
- (9) S. Zhong, S. Odawara, N. G. M. Thao, K. Fujisaki, F. Iwamoto, T. Kimura, and T. Yamada: "Numerical analysis on iron loss of reactor core under hysteresis B-H curve using play model for DC-DC converter," IEEJ Journal of Industry Applications, vol. 9, no. 2, pp. 159-167, 2020.
 - (10) T. Shijo, Y. Uchino, Y. Noda, H. Yamada, and T. Tanaka: "New induction heating coils with reduced iron-loss in the cores for small-foreign-metal particle detector using an SiC-MOSFETs high-frequency inverter," IEEJ Journal of Industry Applications, vol. 8, no. 5, pp. 802-812, 2019.
 - (11) H. Ayano, A. Fujimura, and Y. Matsui: "Improvement of high-frequency characteristics of small-size toroidal reactors with new wire guides," IEEJ Journal of Industry Applications, vol. 8, no. 4, pp. 615-622, 2019.
 - (12) M. Hara, M. Namba, S. Tajima, M. Tani, T. Hattori, and Y. Kaneko: "Properties of iron core fabricated from flaky-shaped and annealed pure iron powder," Materials Transactions, vol. 59, no. 12, pp. 1920-1927, 2018.
 - (13) N. G. M. Thao, K. Fujisaki, L. Ton That, and S. Motozuka: "Magnetic comparison between experimental flake powder and spherical powder for inductor cores at high frequency," IEEE Transactions on Magnetics, vol. 57, no. 2, pp. 1-7, 2021.
 - (14) N. Nakamura, Y. Ozaki, and K. Higuchi: "Flaky-shaped iron powder "KIP MG150D" for soft magnetic applications," Kawasaki Steel Technical Report, no. 47, pp. 60-64, 2002.
 - (15) T. Tosaka, I. Nagano, S. Yagitani, and Y. Yoshimura: "Determining the relative permeability and conductivity of thin materials," IEEE Transactions on Electromagnetic Compatibility, vol. 57, no. 2, pp. 352-360, 2005.
 - (16) O. Suzuki, D. Nagashima, K. Nishimura, and T. Nakagawa: "Magnetic levitation control by considering the twisting mode of a 0.18 mm thick steel plate," IEEE Transactions on Magnetics, vol. 51, no. 11, paper ID: 8600304, 2015.
 - (17) S. Ueno, M. Enokizono, Y. Mori, and K. Yamazaki: "Vector magnetic characteristics of ultra-thin electrical steel sheet for development of high-efficiency high-speed motor," IEEE Transactions on Magnetics, vol. 53, no. 11, paper ID: 6300604, 2017.
 - (18) Y. Fukuda and M. Shimotomai: "Magnetic properties of thin sheets (50 μ m) of Nd-(FeCoNiTi)-B sintered magnets," IEEE Transactions on Magnetics, vol. 9, no. 5, pp. 40-46, 1994.
 - (19) M. Nakano, S. Agatsuma, K. Ishiyama, and K. I. Arai: "(110) [001] grain growth in silicon steel sheets of 30 μ m thickness," IEEE Transactions on Magnetics, vol. 9, no. 1, pp. 67-72, 1994.
 - (20) M. Nakano, K. Ishiyama, and K.L. Arai: "Production of ultra thin grain oriented silicon steel sheets," IEEE Transactions on Magnetics, vol. 31, no. 6, pp. 3886-3888, 1995.
 - (21) Cold rolled steel sheet (TOP), Toyo Kohan Co., Ltd., Japan, [Online] available at: <https://www.toyokohan.co.jp/en/products/top/index.html>
 - (22) DuPont™ Kapton® 20EN polyimide film with thickness of 5 μ m, [Online] available at: www.dupont.com/products/kapton-en.html
 - (23) B-H Analyzer SY-8218 / SY-8219, Iwatsu Electric Co., Ltd., Japan, [Online] available at: www.iti.iwatsu.co.jp/en/pdf/BH_catalog14055E-108.pdf.
 - (24) "Fit curve or surface to data - MATLAB fit", The MathWorks, Inc., Natick, Massachusetts, United States, [Online] available at: www.mathworks.com/help/curvefit/fit.html.
 - (25) R. Ramprasad, P. Zurcher, M. Petras, and M. Miller: "Magnetic properties of metallic ferromagnetic nanoparticle composites", Journal of Applied Physics, vol. 96, no. 1, pp. 519-529, 2004.
 - (26) J. Tateno, T. Hiruta, S. Katsura, A. Honda, T. Miyata, and A. Kamimaru: "Experimental analysis of thickness reduction limits in ultra thin stainless steel foil rolling", ISIJ International, vol. 51, no. 5, pp. 788-792, 2011.
 - (27) N. G. M. Thao, K. Fujisaki, H. Mamiya, S. Kuroda, Y. Mitarai, and N. Motohashi: "Magnetic characterization of 4 μ m-thick steel made by continuous rolling process for power electronic applications in high frequency," Proceedings of the 23rd International Conference on Electrical Machines and Systems (ICEMS 2020), paper ID: LSSH-2, pp. 1031-1034, Hamamatsu, Japan, 2020.

Nguyen Gia Minh Thao (Member) He obtained the B.Eng. (honors) and M.Eng. (first class) degrees in Electrical and Control Engineering from Ho Chi Minh City University of Technology (HCMUT) in 2009 and 2011, respectively. He obtained a Dr.Eng. degree in Electrical Engineering from Waseda University in 2015. From April 2010 to August 2012, he was a Lecturer in the Department of Electrical Machines and Apparatus, HCMUT, Vietnam.



From November 2015 to August 2020, he was a Postdoctoral Research Fellow in Waseda University and Toyota Technological Institute, Japan. He was a designated Assistant Professor in Nagoya University from September 2020 to March 2021. He is presently an Assistant Professor in Toyota Technological Institute. His current research interests include advanced control methods, electric motors and drives, electromagnetic

characterization, high frequency magnetics, power electronics converters, and renewable energy. He is also a member of the Institute of Electrical and Electronics Engineers (IEEE), Asian Control Association (ACA), and Japan Society of Mechanical Engineering (JSME).

Keisuke Fujisaki



(Senior member) He received the B. Eng., M. Eng., and Dr. Eng. degrees in Electronics Engineering from the Faculty of Engineering, The University of Tokyo, Tokyo, Japan, in 1981, 1983, and 1986, respectively. From 1986 to 1991, he conducted research on electromagnetic force applications to steel-making plants at the Ohita Works, Nippon Steel Corporation. From 1991 to 2010, he was a chief researcher in the Technical Development Bureau, Nippon Steel Corporation, Futtsu, Japan. Since 2010, he has been a Professor of Toyota Technological Institute. His current scientific interests are magnetic multi-scale, electromagnetic multi-physics, high efficient motor drive system, electrical motor, and power electronics. In 2002–2003, he was a Visiting Professor at Ohita University. In 2003-2009, he was a Visiting Professor at Tohoku University, Japan. Dr. Fujisaki received the Outstanding Prize Paper Award at the Metal Industry Committee sessions of the 2002 IEEE Industry Applications Society Annual Meeting.

Hiroaki Mamiya



(Non-member) He obtained a Dr. Eng. degree in Applied Physics from the University of Tsukuba in 2002. From 1994, he has been a research scientist in the National Institute for Materials Science (NIMS), Japan. His current scientific interests are magnetism and magnetic materials.

Syuji Kuroda



(Non-member) He is currently with the National Institute for Materials Science (NIMS), in Tsukuba city, Japan.

Yoko Yamabe-Mitarai (Non-member) She is currently with the National Institute for Materials Science (NIMS), in Tsukuba city, Japan.



Norie Motohashi



(Non-member) She is currently with the National Institute for Materials Science (NIMS), in Tsukuba city, Japan.